EFFECTS OF VISCOELASTIC AND POROUS MATERIALS ON SOUND TRANSMISSION OF MULTILAYER SYSTEMS

Hadda Felhi

Laboratory of Mechanics, Modelling and Production (LA2MP), National Engineering School of Sfax, University of Sfax, Sfax, Tunisia, and Faculty of Sciences of Sfax, University of Sfax, Sfax, Tunisia

Hassen Trabelsi

Laboratory of Mechanics, Modelling and Production (LA2MP), National Engineering School of Sfax, University of Sfax, Sfax, Tunisia

Mohamed Taktak

Laboratory of Mechanics, Modelling and Production (LA2MP), National Engineering School of Sfax, University of Sfax, Sfax, Tunisia, and Faculty of Sciences of Sfax, University of Sfax, Sfax, Tunisia
e-mail: mohamed.taktak@fss.rnu.tn

Mabrouk Chaabane

Faculty of Sciences of Sfax, University of Sfax, Sfax, Tunisia

Mohamed Haddar

Laboratory of Mechanics, Modelling and Production (LA2MP), National Engineering School of Sfax, University of Sfax, Sfax, Tunisia

Multilayer structures allow obtaining good performance in acoustic insulation to eliminate unwanted noise in the medium and high frequencies in many applications such as building and transport industry. In this paper, the sound transmission of multilayer systems is studied using the Transfer Matrix Method (TMM). The studied multi-layered panels include elastic, viscoelastic and porous materials. Several configurations of multilayer systems are studied, and their corresponding transmission loss TL is computed. Also, the effects of porous material characteristics are studied to evaluate the impact of each parameter.

Keywords: porous material, multilayer system, transmission loss, transfer matrix

1. Introduction

The control of noise and vibration has become one of the major concerns in several fields of industry (aeronautics, automobile, household appliances...). Indeed, reduction of noise and vibrations avoids material damage and nuisance effects. The use of sandwich systems with a high damping power core is one of ways to reduce elevated noise and vibration levels. This type of structures offers significant technological advantages (low weight, high rigidity, easy automation of manufacturing, etc.). These sandwich panels contain an absorbent porous materials and are widely used in transport and building industries to reduce nuisance noise and improve comfort of individuals.

In order to increase acoustic insulation properties of multilayer panel configurations, elastic, viscoelastic and porous materials were studied by Allard *et al.* (1987), Mueller and Tschudl (1989), Atalla *et al.* (1998), Ghinet *et al.* (2005) and Abid *et al.* (2012). The behavior of panel combinations of materials depends more or less on dimensions and boundary conditions of edges. Nevertheless, interesting results can be obtained by modeling the samples in the form of infinite plates subjected to incident plane waves.

The modeling of the acoustic response of multilayer structures is done using different methods. Tanneau (2004) and Tanneau *et al.* (2006) studied modeling of an aeronautical insulation panel by the finite elements and boundary elements. These methods are applicable in low frequencies. When the frequency domain increases, the implementation of these methods is confronted with an excessive increase of the degrees of freedom associated with fineness of the mesh compatible with wavelengths. The cost of calculations becomes then prohibitive and the results are very sensitive to the least perturbation of geometric and physical parameters. In order to overcome these disadvantages, Thomson (1950), Allard *et al.* (1989), Lee and Xu (2009), Munjal (1993) and Sastry and Munjal (1995) presented an analytical method for the estimation of acoustic indicators of stratified media called the Transfer Matrix Method (TMM). This method is based on the representation of propagation of plane waves in different media in terms of the transfer matrix.

The TMM is applied with an excitation of the air (normal or oblique acoustic wave) and in a diffuse field. The TMM is based on calculation of the transfer matrix of each layer. These matrices are obtained by applying continuity conditions on the interfaces between layers giving a system of equations linking speeds and stresses between the layers. The global transfer matrix is calculated: If the layers are of the same nature, the transfer matrix is made by multiplying the transfer matrix of each layer. If the layers are different, the interface matrix is used. Finally, the transmission loss TL is calculated from the resulting global transfer matrix as presented by Munjal *et al.* (1993).

The aim of the present paper is to predict the acoustic parameters of several multilayer configurations by the Transfer Matrix Method and to study also the effect of replacement of the viscoelastic layer instead of the elastic solid layer. Also, the effects of porous parameters on the behavior of sound transmission of these configurations are studied in order to improve the acoustic insulation of multilayer panels.

The outline of the document is as follows: Section 1 presents description of the TMM for predicting the transfer matrix of a multilayer structure. In Section 2, calculation of the transmission loss from the obtained transfer matrix is presented. Finally, numerical results and a comparison study based on the replacement of the elastic layer by a viscoelastic layer are presented in Section 3. In this Section, a parametric study is carried out to choose the best multilayer configuration.

2. The transfer matrix method

2.1. General formulation

The transfer matrix method is based on the modeling of propagation of plane waves in various layers by the transfer matrix. As presented in Fig. 1, the studied layer is an h thickness layer excited by an oblique wave plane. The geometry of the problem is bidimensional in the incident plane (x_1, x_3). The lateral dimension of the layer is supposed to be infinite. Various types of waves can propagate in the material according to their nature as studied by Allard and Atalla (2009). The sound propagation in the layer is represented by a transfer matrix $\mathbf{T}$ as follows

$$\mathbf{V}_{M_1} = \mathbf{T}\mathbf{V}_{M_2} \tag{2.1}$$

where M_1 and $M2$ are sets close to the forward and backward face of the layer, respectively, and where the components of the vector $\mathbf{V}_{M_1}$ and $\mathbf{V}_{M_2}$ are respectively the variables which describe the acoustic field at the points M_1 and M_2 of the medium. The transfer matrix $\mathbf{T}$ depends on the thickness h and the acoustical properties of each medium.
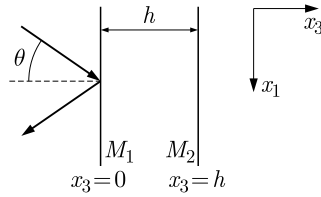
Fig. 1. Layer subjected to an oblique incident wave

2.2. Construction of the transfer matrix

Figure 2 represents a multi-layer structure composed of solid and poroelastic layers. In the following, the computation of the transfer matrix of each medium is presented.
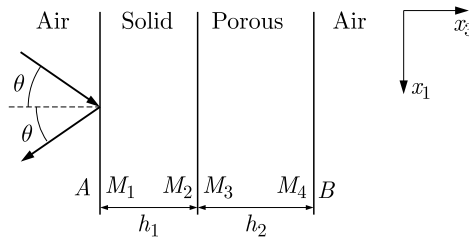

Fig. 2. Multilayered panel

2.2.1. Solid layer

In an elastic solid layer, longitudinal and shear waves propagate into the layer. The acoustic field in the material is described using the amplitudes of the following waves: the incident and reflected longitudinal waves and the incident and reflected shear waves (A_1, A_2, A_3 and A_4). The associated displacement potentials can be written as follows

$$\phi = \exp(\mathrm{j}wt - \mathrm{j}k_1 x_1)[A_1 \exp(-\mathrm{j}k_{13} x_3) + A_2 \exp(\mathrm{j}k_{13} x_3)]$$
$$\psi = \exp(\mathrm{j}wt - \mathrm{j}k_1 x_1)[A_3 \exp(-\mathrm{j}k_{33} x_3) + A_4 \exp(\mathrm{j}k_{33} x_3)]$$

(2.2)

where the x_3 components k_{13} and k_{33} of the wave number vectors are expressed as follows

$$k_{13} = \sqrt{\delta_1^2 - k_t^2} \qquad k_{33} = \sqrt{\delta_3^2 - k_t^2}$$

(2.3)

The x_1 component of the wave number k_1 is given by

$$k_1 = k \sin \theta$$

(2.4)

δ_1^2 and δ_3^2 are respectively the squares of the wave numbers of the longitudinal and shear waves in the elastic solid layer. They are given by

$$\delta_1^2 = \frac{\omega^2 \rho_s}{\lambda + 2\mu} \qquad \delta_3^2 = \frac{\omega^2 \rho_s}{\mu}$$

(2.5)

where ρ_s is the surface density of the elastic solid, λ and μ are, respectively, the first and second Lamé coefficients. The acoustic field in the elastic solid layer can be predicted if the amplitudes A_1, A_2, A_3 and A_4 are known. Instead of these parameters, four mechanical variables may be known to express sound propagation everywhere in the medium. Following Folds and Loggins (1977) the four chosen quantities are v_1^s and v_3^s being respectively the x_1 and x_3 components

of the velocity at point M_i as well as σ_{33}^s and σ_{13}^s being respectively the normal and tangential stresses at the point M_i. The vector $\mathbf{V}^s$ in this case is expressed as follows

$$\mathbf{V}_{M_i}^s = [\nu_1^s(M_i), \nu_3^s(M_i), \sigma_{33}^s(M_i), \sigma_{13}^s(M_i)]^\mathrm{T} \qquad i = 1, 2 \tag{2.6}$$

These velocities and stresses are written as follows

$$\nu_1^s = \mathrm{j}\omega\Big(\frac{\partial\phi}{\partial x_1} - \frac{\partial\psi}{\partial x_3}\Big) \qquad \nu_3^s = \mathrm{j}\omega\Big(\frac{\partial\phi}{\partial x_3} + \frac{\partial\psi}{\partial x_1}\Big)$$
$$\sigma_{33}^s = \lambda\Big(\frac{\partial^2\phi}{\partial x_1^2} + \frac{\partial^2\phi}{\partial x_3^2}\Big) + 2\mu\Big(\frac{\partial^2\phi}{\partial x_3^2} + \frac{\partial^2\psi}{\partial x_1\partial x_3}\Big) \qquad \sigma_{13}^s = \mu\Big(2\frac{\partial^2\phi}{\partial x_1\partial x_3} + \frac{\partial^2\psi}{\partial x_1^2} - \frac{\partial^2\psi}{\partial x_3^2}\Big) \tag{2.7}$$

To obtain the transfer matrix $\mathbf{T}^s$ of the elastic solid layer, the vector $\mathbf{V}_{M_1}^s$ is first connected to the amplitudes of different waves propagating in the layer presented by the following vector

$$\mathbf{A} = [(A_1 + A_2), (A_1 - A_2), (A_3 + A_4), (A_3 - A_4)] \tag{2.8}$$

and by the matrix $\mathbf{\Gamma}(x_3)$ such that

$$\mathbf{V}_M^s = \mathbf{\Gamma}(x_3)\mathbf{A} \tag{2.9}$$

If the origin of the x_3 axis is fixed at the point M_i, the vectors $\mathbf{V}_{M_1}^s$ and $\mathbf{V}_{M_2}^s$ are expressed as

$$\mathbf{V}_{M_1}^s = \mathbf{\Gamma}(0)\mathbf{A} \qquad \mathbf{V}_{M_2}^s = \mathbf{\Gamma}(h)\mathbf{A} \tag{2.10}$$

Then, the transfer matrix $\mathbf{T}^s$ which relates $\mathbf{V}_{M_1}^s$ and $\mathbf{V}_{M_2}^s$ is equal to

$$\mathbf{T}^s = \mathbf{\Gamma}(0)\mathbf{\Gamma}^{-1}(h) \tag{2.11}$$

2.2.2. Poroelastic layer

In a porous material structure, three elastic waves propagate into the medium: two compression waves and a shear wave (Allard *et al.*, 1987). The displacement potential of the compression ϕ^s and shear ψ^s waves are given by

$$\phi_1^s = \exp(\mathrm{j}\omega t - \mathrm{j}k_1 x_1)[A_1 \exp(-\mathrm{j}k_{13}x_3) + A_1' \exp(\mathrm{j}k_{13}x_3)]$$
$$\phi_2^s = \exp(\mathrm{j}\omega t - \mathrm{j}k_1 x_1)[A_2 \exp(-\mathrm{j}k_{23}x_3) + A_2' \exp \mathrm{j}k_{23}x_3)] \tag{2.12}$$
$$\psi_2^s = \exp(\mathrm{j}\omega t - \mathrm{j}k_1 x_1)[A_3 \exp(-\mathrm{j}k_{33}x_3) + A_3' \exp(\mathrm{j}k_{33}x_3)]$$

The air displacement potentials are related to the layer displacement potentials by

$$\phi_i^f = \mu_i\phi_i^s \qquad i = 1, 2 \qquad \psi_1^f = \mu_3\phi_2^s \tag{2.13}$$

with

$$\frac{\phi_i^f}{\phi_i^s} = \frac{P\delta_i^2 - \omega^2\widetilde{\rho}_{11}}{\omega^2\rho_{12} - Q\delta_i^2} \qquad i = 1, 2 \qquad \mu_3 = -\frac{\widetilde{\rho}_{12}}{\rho_{22}}$$

The ratio μ_i of the velocity of the air over the velocity of the frame is for two compression waves and μ_3 is for the shear wave. The acoustic field in the porous layer can be predicted everywhere if the six amplitudes A_1, A_1', A_2, A_2', A_3, A_3' are known. However, instead of these parameters, six independent acoustic quantities can be chosen. Three velocity components and three elements of the stress tensors: two velocity components ν_1^s and ν_3^s of the frame, the velocity component ν_3 of the fluid, two components σ_{33}^s and σ_{13}^s of the stress tensor of the frame and σ_{33}^f in the fluid. If these six quantities are known at the point M_i in the layer, the acoustic field can be predicted

everywhere in the layer. Moreover, the values of these quantities anywhere in the layer depend linearly on the values of these quantities at M_i. So, the vector $\mathbf{V}^p_{M_i}$ can be defined as follows

$$\mathbf{V}^p_{M_i} = [\nu^s_1(M_i), \nu^s_3(M_i), \nu^f_3(M_i), \sigma^s_{33}(M_i), \sigma^s_{13}(M_i), \sigma^f_{33}(M_i)]^{\mathrm{T}} \tag{2.14}$$

$\mathbf{V}^p_{M_i}$ being a column vector. These six quantities are written as

$$\nu^s_1 = \mathrm{j}\omega\Big(\frac{\partial\phi^s_1}{\partial x_1} + \frac{\partial\phi^s_2}{\partial x_1} - \frac{\partial\psi^s_2}{\partial x_3}\Big) \qquad \nu^k_3 = \mathrm{j}\omega\Big(\frac{\partial\phi^k_1}{\partial x_3} + \frac{\partial\phi^k_2}{\partial x_3} - \frac{\partial\psi^k_2}{\partial x_1}\Big) \qquad k = s, f$$

$$\sigma^s_{33} = (P - 2N)\Big(\frac{\partial^2(\phi^s_1 + \phi^s_2)}{\partial x^2_1} + \frac{\partial^2(\phi^s_1 + \phi^s_2)}{\partial x^2_3}\Big) + Q\Big(\frac{\partial^2(\phi^f_1 + \phi^f_2)}{\partial x^2_1} + \frac{\partial^2(\phi^f_1 + \phi^f_2)}{\partial x^2_3}\Big)$$

$$\qquad + 2N\Big(\frac{\partial^2(\phi^s_1 + \phi^s_2)}{\partial x^2_3} + \frac{\partial^2\psi^2_2}{\partial x_1 \partial x_3}\Big) \tag{2.15}$$

$$\sigma^s_{13} = N\Big(2\frac{\partial^2(\phi^2_1 + \phi^2_2)}{\partial x_1 \partial x_3} + \frac{\partial^2\psi^s_2}{\partial x^2_1} - \frac{\partial^2\psi^s_2}{\partial x^2_3}\Big)$$

$$\sigma^f_{33} = R\Big(\frac{\partial^2(\phi^f_1 + \phi^f_2)}{\partial x^2_1} + \frac{\partial^2(\phi^f_1 + \phi^f_2)}{\partial x^2_3}\Big) + Q\Big(\frac{\partial^2(\phi^s_1 + \phi^s_2)}{\partial x^2_1} + \frac{\partial^2(\phi^s_1 + \phi^s_2)}{\partial x^2_3}\Big)$$

where N is the shear modulus of the material, and P, Q and R are the elastic coefficients of Biot (Biot, 1956).

The vector $\mathbf{V}^p_{M_i}$ satisfies the relation

$$\mathbf{V}^p_{M_i} = \mathbf{\Gamma}(x_3)\mathbf{A} \tag{2.16}$$

with $\mathbf{A}$ being the column vector defined as

$$\mathbf{A} = [(A_1 + A'_1), (A_1 - A'_1), (A_2 + A'_2), (A_2 - A'_2), (A_3 + A'_3), (A_3 - A'_3)]^{\mathrm{T}} \tag{2.17}$$

and $\mathbf{\Gamma}(x_3)$ is a connectivity matrix which results from system (2.12). As in the case of a solid layer, the transfer matrix between two points is obtained by the same procedure

$$\mathbf{T}^p = \mathbf{\Gamma}(0)\mathbf{\Gamma}(h^{-1}) \tag{2.18}$$

2.2.3. Viscoelastic layer

Mechanical characteristics of viscoelastic materials depend on the excitation frequency. To describe such a material, the complex representation of the Young modulus following (Abid *et al.*, 2012; Szabo, 2000; Soula and Chevalier, 1998) is used

$$E^* = E_0\frac{1 + \mathrm{j}\omega\tau_u}{1 + \mathrm{j}\omega\tau} \tag{2.19}$$

and

$$E' = E_0\frac{1 + \tau\tau_u\omega^2}{1 + w^2\tau^2} \qquad E'' = E_0\frac{\omega(\tau_u - \tau)}{1 + w^2\tau^2} \tag{2.20}$$

where E' and E'' are respectively the real and imaginary parts of the complex modulus E_0, τ and τ_u are relaxation times of the viscoelastic material determined experimentally with relaxation and creep tests.

2.3. Continuity relations at the interfaces

The objective of this Section is to examine continuity relations for all possible interfaces. These relations depend on the nature of materials of the adjacent layers (Allard *et al.*, 1989).

2.3.1. Fluid-solid interface

The continuity conditions are given by

$$-p(A) = \sigma_{33}^s(M_1) \qquad\qquad 0 = \sigma_{13}^s(M_1) \qquad\qquad \nu_3^f(A) = \nu_3^s(M_1) \qquad\qquad (2.21)$$

The following equations can be condensed as follows

$$\mathbf{I}_{f,s}\mathbf{V}(A) + \mathbf{J}_{f,s}\mathbf{V}(M_1) = \mathbf{0} \qquad\qquad (2.22)$$

with

$$\mathbf{I}_{f,s} = \begin{bmatrix} 0 & -1 \\ 1 & 0 \\ 0 & 0 \end{bmatrix} \qquad\qquad \mathbf{J}_{f,s} = \begin{bmatrix} 0 & 1 & 0 & 0 \\ 0 & 0 & 1 & 0 \\ 0 & 0 & 0 & 1 \end{bmatrix} \qquad\qquad (2.23)$$

$\mathbf{J}_{f,s}$ and $\mathbf{I}_{f,s}$ must be interchanged for the fluid-solid interface.

2.3.2. Porous-fluid interface

The continuity conditions are given by

$$(1 - \phi)\nu_3^s(M_4) + \phi\nu_3^f(M_4) = \nu_3^f(B)$$
$$\sigma_{33}^f(M_4) = -\phi p(B) \qquad\qquad \sigma_{33}^s(M_4) = -(1 - \phi)p(B) \qquad\qquad \sigma_{13}^s(M_4) = 0 \qquad\qquad (2.24)$$

where ϕ is the porosity of the porous layer. These equations can be rewritten in the form

$$\mathbf{I}_{p,f}\mathbf{V}_{M_4}^p + \mathbf{J}_{p,f}\mathbf{V}_B^f = \mathbf{0} \qquad\qquad (2.25)$$

with

$$\mathbf{I}_{p,f} = \begin{bmatrix} 0 & 1-\phi & \phi & 0 & 0 & 0 \\ 0 & 0 & 0 & 1 & 0 & 0 \\ 0 & 0 & 1 & 0 & 1 & 0 \\ 0 & 0 & 0 & 0 & 0 & 1 \end{bmatrix} \qquad\qquad \mathbf{J}_{p,f} = \begin{bmatrix} 0 & -1 \\ -\phi & 0 \\ 0 & 0 \\ \phi & 0 \end{bmatrix} \qquad\qquad (2.26)$$

The matrices $\mathbf{I}_{p,f}$ and $\mathbf{J}_{p,f}$ must be interchanged for the fluid-porous interface.

2.3.3. Solid-porous interface

The continuity conditions are given by

$$\nu_3^s(M_2) = \nu_3^s(M_3) = \nu_3^f(M_3) \qquad\qquad \nu_1^s(M_2) = \nu_1^s(M_3)$$
$$\sigma_{13}^s(M_2) = \sigma_{13}^s(M_3) \qquad\qquad \sigma_{33}^s(M_2) = \sigma_{33}^f(M_3) + \sigma_{33}^s(M_3) \qquad\qquad (2.27)$$

This can be rewritten as follows

$$\mathbf{I}_{s,p}\mathbf{V}_{M_2}^s + \mathbf{J}_{s,p}\mathbf{V}_{M_3}^p = \mathbf{0} \qquad\qquad (2.28)$$

where

$$\mathbf{I}_{s,p} = \begin{bmatrix} 1 & 0 & 0 & 0 \\ 0 & 1 & 0 & 0 \\ 0 & 1 & 0 & 0 \\ 0 & 0 & 1 & 0 \\ 0 & 0 & 0 & 1 \end{bmatrix} \qquad\qquad \mathbf{J}_{s,p} = \begin{bmatrix} 1 & 0 & 0 & 0 & 0 & 0 \\ 0 & 1 & 0 & 0 & 0 & 0 \\ 0 & 0 & 1 & 0 & 0 & 0 \\ 0 & 0 & 0 & 1 & 0 & 1 \\ 0 & 0 & 0 & 0 & 1 & 0 \end{bmatrix} \qquad\qquad (2.29)$$

The matrices $\mathbf{I}_{s,p}$ and $\mathbf{J}_{s,p}$ must be interchanged for the porous-solid interface.
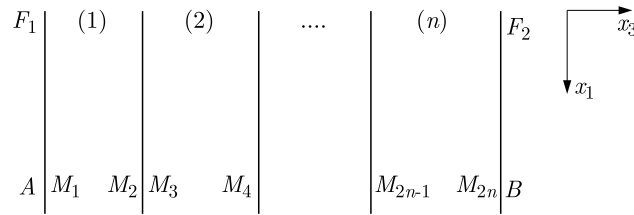
Fig. 3. A multilayer domain

2.4. Computation of the transmission loss TL of the multilayer

Generally way, the expressions of continuity between all layers of the system as presented in Fig. 3, are written by the following intermediate equations

$$\mathbf{I}_{f,1}\mathbf{V}_A^f + \mathbf{J}_{f,1}\mathbf{V}_{M_2}^1 = \mathbf{0}$$
$$\mathbf{I}_{k,k+1}\mathbf{V}_{M_{2k}}^k + \mathbf{J}_{k,k+1}\mathbf{T}^k\mathbf{V}_{M_{2(k+1)}}^k = \mathbf{0} \qquad k = 1,\ldots,n-1 \tag{2.30}$$

This set of equations can be rewritten as

$$\mathbf{D}\mathbf{V}_0 = \mathbf{0} \tag{2.31}$$

where

$$\mathbf{D} = \begin{bmatrix} \mathbf{I}_{f,1} & \mathbf{J}_{f,1}\mathbf{T}^1 & 0 & 0 & 0 \\ 0 & \mathbf{I}_{1,2} & \mathbf{J}_{1,2}\mathbf{T}^2 & 0 & 0 \\ \cdots & \cdots & \cdots & \cdots & \cdots \\ 0 & 0 & \mathbf{I}_{(n-2)(n-1)} & \mathbf{J}_{(n-2)}\mathbf{T}^{n-1} & 0 \\ 0 & 0 & 0 & \mathbf{I}_{(n-1)(n)} & \mathbf{J}_{(n-1)(n)} \end{bmatrix} \tag{2.32}$$
$$\mathbf{V}_0 = [V_A^f, V_{M_2}^1, V_{M_1}^2, \ldots, V^{(n-1)}(M_{2n-1}), V^{(n)}(M_{2n}), V_B^f]^{\mathrm{T}}$$

Then, D' and D'' matrices are defined as follows

$$\mathbf{D}' = \begin{bmatrix} -1 & \cdots & \mathbf{D} & \cdots & 0 \\ \cdots & \cdots & \cdots & \cdots & \cdots \\ 0 & \cdots & 0 & -1 & Z_B \end{bmatrix} \qquad \mathbf{D}'' = \begin{bmatrix} -1 & Z_A & 0 & \cdots & 0 \\ \cdots & \cdots & \mathbf{D} & \cdots & \cdots \\ 0 & \cdots & 0 & -1 & Z_B \end{bmatrix} \tag{2.33}$$

such as

$$\mathbf{D}'\mathbf{V}_0 = \mathbf{0} \tag{2.34}$$

where Z_A and Z_B are, respectively, the impedance of the medium A and B.

The determinant of the matrix $\mathbf{D}''$ must be equal to zero. Z_A is given by

$$Z_A = -\frac{|\mathbf{D}'|}{|\mathbf{D}'_2|} \tag{2.35}$$

where $|\mathbf{D}'_1|$ is the determinant of the matrix $\mathbf{D}'$ without its first column, $|\mathbf{D}'_2|$ is the determinant of the matrix $\mathbf{D}'$ without its second column.

The reflection coefficient R is related to Z_A by

$$R = \frac{Z_A - \frac{Z_C}{\cos\theta}}{Z_A + \frac{Z_C}{\cos\theta}} \tag{2.36}$$

where Z_C is the characteristic impedance in the air medium

$$Z_C = \rho_{air} C_{air} \tag{2.37}$$

The transmission coefficient T is determined as follows

$$T = (1 + R) \frac{|\mathbf{D}'_{N-1}|}{|\mathbf{D}'_1|} \tag{2.38}$$

where $|\mathbf{D}'_{N-1}|$ is the determinant of $\mathbf{D}'$ without the $(N-1)$ column.

The TL transmission loss is defined by

$$TL = 10 \log \frac{1}{\tau} \tag{2.39}$$

where τ is the acoustic transparency defined as follows

$$\tau = \frac{P_T}{P_I} \tag{2.40}$$

The symbols P_T, P_I represent, respectively, the transmitted and the incident power waves, and finally

$$TL = 10 \log \frac{P_I}{P_T} = 10 \log \frac{\frac{p_i^2}{2Z_{fluid1}}}{\frac{p_t^2}{2Z_{fluid2}}} \tag{2.41}$$

where p_i, p_t represent, respectively, the amplitude of the incident and the transmitted waves.

3. Numerical results

3.1. Validation of the TMM

The TMM is tested by comparing its results with experimental findings obtained by Tanneau (2004). Two configurations are studied:
- The first is a 2.1 mm thickness plate glued to to 30 mm thick porous material.
- The second is composed by the 30 mm thick porous material glued to two 2.1 mm thick plates on each side. The mechanical proprieties of the used materials are presented in Table 1.

Table 1. Parameters of tested materials

Parameters	Porous	Plate
Porosity φ_p	0.98	–
Tortuosity α_∞	1.03	–
Resistivity σ_p [Ns/m^4]	6600	–
Viscous length Λ [μm]	200	–
Thermal length Λ' [μm]	380	–
Density ρ [kg/m^3]	11.2	1100
Poisson's coefficient ν	0.3	0.3
Young's modulus E [Pa]	292.8e3	2.62e9
Damping loss factor η	0.0624	0.06

Figures 4a and 4b represent, respectively, a comparison between the computed and the experimental TL obtained in the two studied configurations and for the incident angle $\theta = \pi/4$. A good agreement is observed between the results obtained by the TMM and the experimental results (Tanneau, 2004; Tanneau *et al.*, 2006). In these figures, we can distinguish 3 zones:
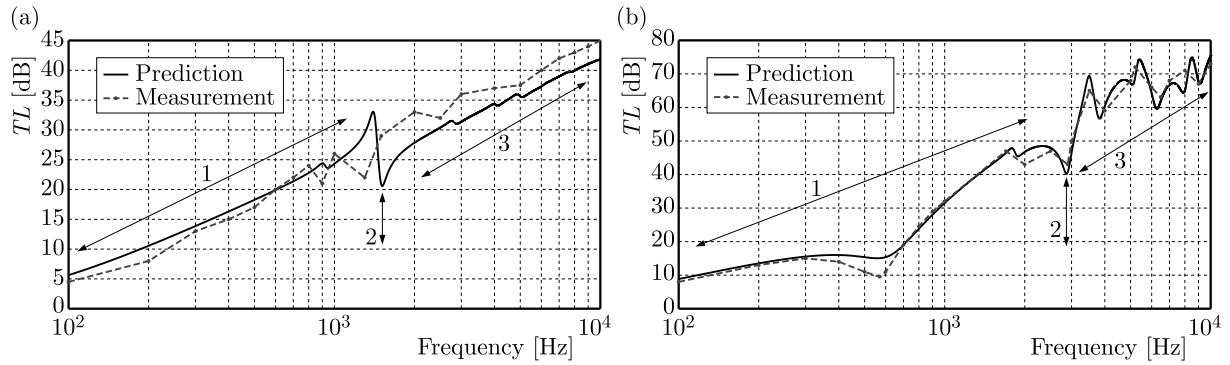
Fig. 4. Theoretical and experimental transmission loss TL of the studied (a) plate-porous configuration and (b) plate-porous-plate configuration

- zone 1: $f < f_{coin}$ – the mass controls the transmission. The wavelength in this frequency range is very large compared to the thickness of the wall. For this, the behavior of the multi-layer wall will be identical to that of a simple wall; therefore, the slope of the transmission will be of $6\,\mathrm{dB/octave}$
- zone 2: $f = f_{coin}$ – the damping plays a significant role
- zone 3: $f > f_{coin}$ – the stiffness controls the transmission.

where f_{coin} is the coincidence frequency. It is the frequency at which the airborne acoustic wavelength matches the plate bending wavelength. It is expressed as follows

$$f_{coin} = \frac{c^2}{2\pi \sin^2 \theta} \sqrt{\frac{12\rho(1 - \nu^2)}{Eh^2}} \tag{3.1}$$

Also, comparison between the coincidence frequencies as presented in Tables 2 and 3 showed a good agreement.

Table 2. Comparison between the theoretical and experimental coincidence frequencies in the case of plate-porous configuration

TMM	Theoretical (London, 1950)	Experimental (Tanneau, 2004)
1643 Hz	1554.7 Hz	1450 Hz

Table 3. Comparison between the theoretical and experimental coincidence frequencies in the case of plate-porous-plate configuration

TMM	Theoretical (London, 1950)	Experimental (Tanneau, 2004)
2987 Hz	3317.8Hz	3000 Hz

Results presented in Figs. 4a and 4b and Tables 2 and 3 allow validation of the proposed method (TMM).

3.2. Response of multilayer systems

In this part, the TMM is used to compute the TL of several multilayer configurations to find the best arrangement of layers in terms of sound transmission. Two configurations are studied which are:

- First configuration: 1 mm of the elastic layer – 30 mm of the porous layer.
- Second configuration: 0.5 mm of the elastic layer – 30 mm of the porous layer – 0.5 mm of the elastic layer.

The two studied configurations are subjected to an incident wave at $\theta = \pi/4$. The characteristics of the porous and the elastic layers are respectively presented in Table 4.

Table 4. Parameters of the used materials

Parameters	Foam	Steel
Porosity φ_p	0.98	–
Tortuosity α_∞	1.03	–
Resistivity σ_p [Ns/m^4]	6600	–
Viscous length Λ [μm]	200	–
Thermal length Λ' [μm]	380	–
Density ρ [kg/m^3]	11.2	7850
Poisson's coefficient ν	0.3	0.3
Young's modulus E [Pa]	292.8e3	210e9
Damping loss factor η	0.0624	0.06

The predicted transmission loss TL is presented in Fig. 5. For the first configuration, it is seen that the evaluation of the TL with frequency is progressive but it presents a weak peak at the frequency 1500 Hz.
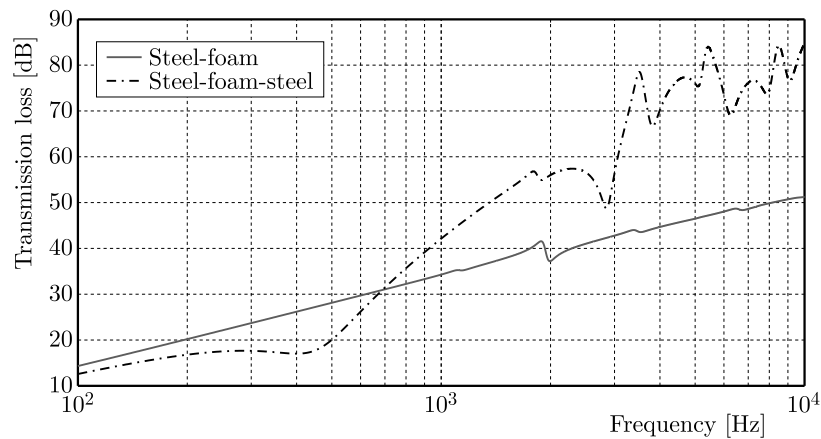

Fig. 5. Comparison of TL versus frequency curves amongst double and triple panel

For the second configuration, the TL is less important for the low frequency up to 450 Hz, then it successively increases with frequency. At high frequencies, the TMM is able to predict the TL with good accuracy. The thickness resonance at 2900 Hz is well predicted. This curve has a high-frequency discontinuous track corresponding to the coincidence zone.

As seen in Fig. 5, the TL value for the first configuration does not exceed 52 dB, on the other hand, for the second configuration, which includes three layers, the TL value reaches 85 dB at high frequencies, which may be explained by the effect of the elastic layer. It is found that the second configuration with triple layers has good insulation behavior, especially in the high frequency range 700 Hz-10000 Hz.

In comparison between the two studied configurations, it seems that the second configuration isolates better than the first configuration.

3.2.1. *Effect of replacing the steel layer by a viscoelastic layer*

In this Section, the steel layers in the two studied configurations are replaced by viscoelastic layers and conserving the same weight of each configuration to show the effect of this replacement. The mechanical proprieties of the viscoelastic layer are presented in Table 5. To have the same mass after replacing the elastic layer, the dimension of the viscoelastic layer must be changed. In fact, thickness of the viscoelastic layer equivalent to the same mass is

$$e = \frac{7850 \cdot 1}{950} = 8.26 \, \text{mm} \tag{3.2}$$

Table 5. Mechanical properties of the viscoelastic layer

E_0 [MPa]	E_∞ [MPa]	f_{carac}	ρ [kg/m^3]	ν
10	100	1000	950	0.49

The viscoelastic material behaves as if it was elastic respectively with the moduli:

- E_∞: at high frequency
- E_0: low frequency
- f_{carac}: is the frequency of the maximum of damping.

Figure 6 presents the TL when using the viscoelastic layers. For the double layer structure, the presented results show that in the low frequency region the same behavior is observed. The response is governed by the mass law, although we have the same excitation and mass. It is also noted that the small difference from the frequency 4000 Hz is due to contribution of the viscoelastic layer.
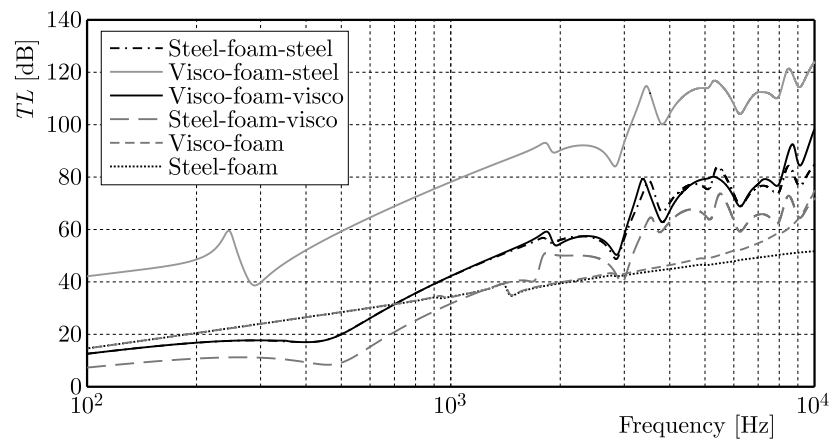

Fig. 6. Comparison between studied configurations

For the 2nd structure, the replacement of the elastic layer by a viscoelastic one generates four cases:

1) viscoelastic-porous-elastic
2) viscoelastic-porous-viscoelastic
3) elastic-porous-elastic
4) elastic-porous-viscoelastic

It is observed that adding the viscoelastic layer leads to a clear difference between these four cases: TL significantly changes when the plane wave penetrates the viscoelastic medium. If the incident wave penetrates first the viscoelastic medium it is seen that the sound insulation is very high. Also, it is observed that the peak of the frequency of coincidence moves to the low frequency range.

Finally, these comparisons show an improvement of the sound insulation for three-layer configurations, especially that one which takes the viscoelastic layer and the steel layer to extremity. This is explained by the damping effect of the viscoelastic material.

3.2.2.   Effect of angle of incidence

Figure 7 shows the attenuation index TL according to the frequency computed for four angles of incidence. The results show that the acoustic transparency strongly depends on the angle of incidence. It is observed that when the incident angle increases, the TL increases. The coincidence frequencies move to the high frequency range as the angle increases.
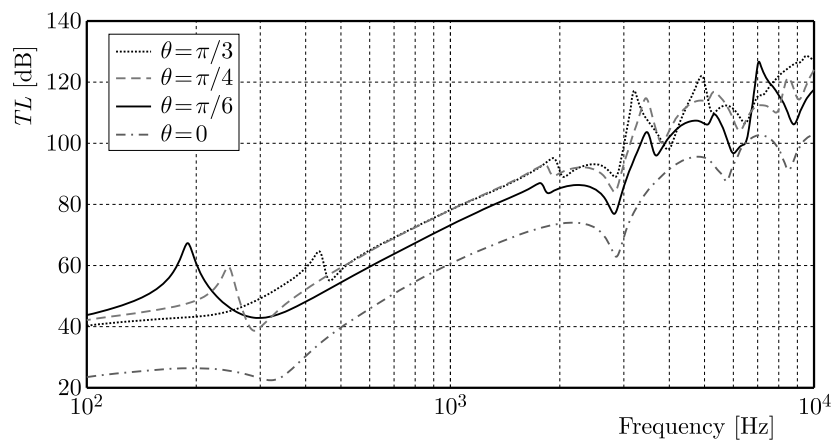

Fig. 7. Effect of the angle of incidence for the configuration (viscoelastic-porous-elastic)

However, we can notice a singular difference at the critical frequency particularly clear for $\theta = 0$.

On the other hand, in Fig. 8, it is clearly observed that the TL is less important if the angle of incidence increases, but the frequency of coincidence retains almost the same position.

As we have seen in the two configurations, the variations in the angle of incidence are not the same. This explains why the viscoelastic layer depends on the angle of excitation.
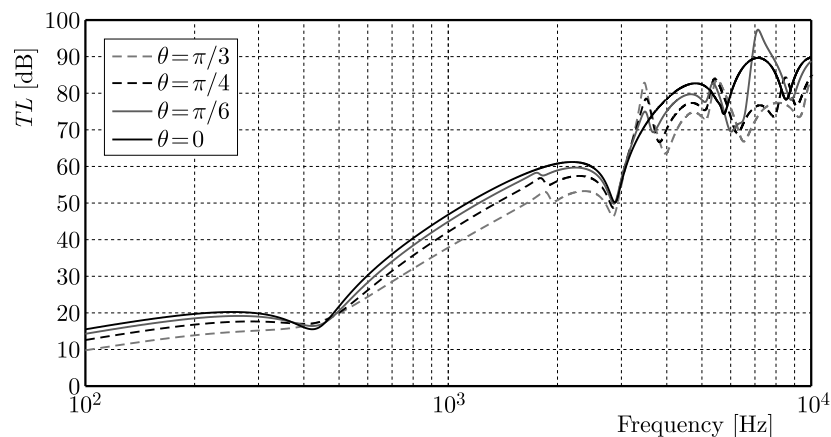

Fig. 8. Effect of the angle of incidence for the configuration (elastic-porous-elastic)

4. Parametric study

In this part, we will choose the configuration which isolates much better than other configurations (viscoelastic-porous-elastic). We are interested in the effect of the porous parameters on the TL of this multilayer structure. The Allard model is used to describe the porous materials. Eight parameters are used: porosity, tortuosity, flux resistivity, viscous lengths and lengths of thermal characteristics, Young's modulus and Poisson's coefficient. The influence of each of these physical parameters on the loss of transmission is studied and discussed in the following Section.

Influence of porosity. Figure 9a presents the effect of porosity – there is no clear influence on the TL of the studied configuration in low frequency band but the higher is porosity, the more absorbent is the material in high frequencies.

Influence of tortuosity. Figure 9b presents the effect of tortuosity – it is seen that an increase in the tortuosity increases the TL just in the high frequency region 1800 Hz-10000 Hz. Tortuosity mainly affects the location of the quarter-wavelength peaks.

Influence of density of the skeleton. As presented in Fig. 10a, if density of the skeleton increases, there will be a shift of the absorption peaks to the low frequency area and the absorption peaks are large. Moreover, density of this material is considered to be an important factor that governs the sound absorption behavior of the material. At the same time, the cost of an acoustical material is directly related to its density.

Influence of Young's modulus. Figure 10b shows that an increase of Young's modulus of the skeleton generates an increase in the rigidity of the skeleton over which the absorption peaks shift to the high frequency area. In our study, we focus on the influence of the porous layer of sound insulation of sandwich plates in the frequency range 100 Hz-10000 Hz, for this reason, we chose Young's modulus for the skeleton of the order of 0.1 MP.

Influence of characteristic length. Figure 11a presents the effect of characteristic length. In the frequency range between 100 Hz-250 H,z the characteristic length has no effects on the TL. In the frequency range 300 Hz-2500 Hz, the more characteristic length decreases, the more viscous dissipation is important, and TL increases. At high frequencies, characteristic lengths represent no effects on the TL.

Influence of resistivity. The variation of the flow resistivity has no effect on the reduction index as presented in Fig. 11b.

Influence of Poisson's ratio. Figure 12a shows the effect of Poisson's ratio on TL. In the frequency band 100 Hz-220 Hz, an increase in the coefficient occurs at an increase in the transmission loss TL. On the contrary, in the frequency band 220 Hz-5000 Hz, this frequency range shows a drop of TL down to 980 Hz, called the resonance frequency, and in the zone 5000 Hz-10000 Hz, if the Poisson ratio is increased, the transmission loss increases. Then, the more Poisson's ratio increases, the more the shear modulus decreases and the more absorption peaks are shifted towards the high-frequency zone.

Influence of foam thickness. For thickness variation of the order of a few millimeters (Fig. 12b), the greater the thickness, the more the transmission loss coefficient increases in the high frequency zone 180 Hz-10000 Hz and the more the absorption peaks is shifted to the low-frequency area. A greater thickness allows a shock-absorbing effect in the behavior of the multilayer.
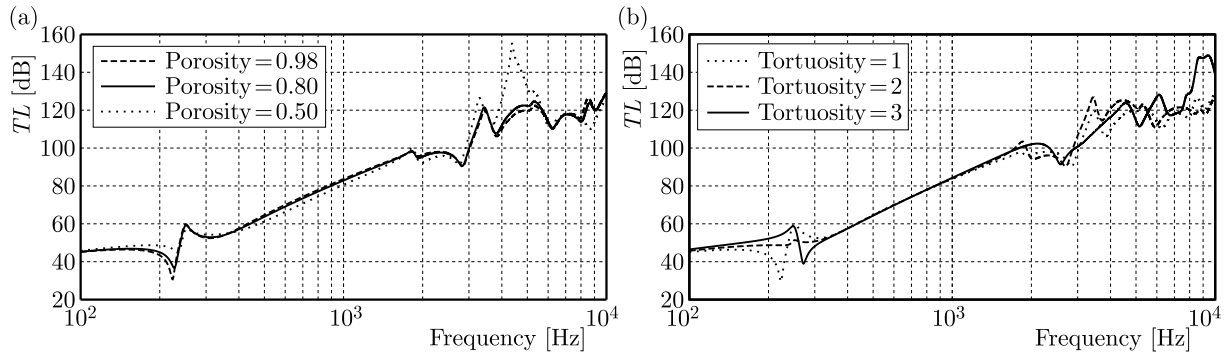
Fig. 9. Influence of (a) porous material porosity and (b) porous material tortuosity on TL of the viscoelastic-porous-elastic configuration
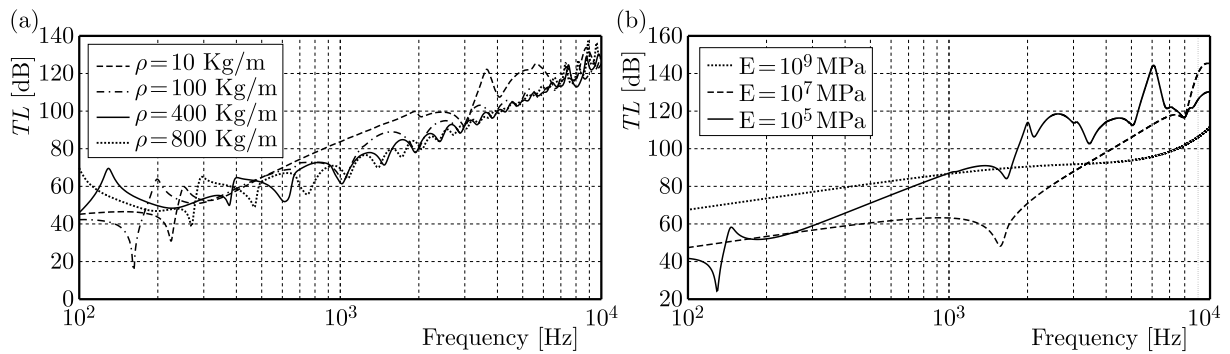

Fig. 10. Influence of (a) porous skeleton density and (b) Young's modulus on TL of the viscoelastic-porous-elastic configuration
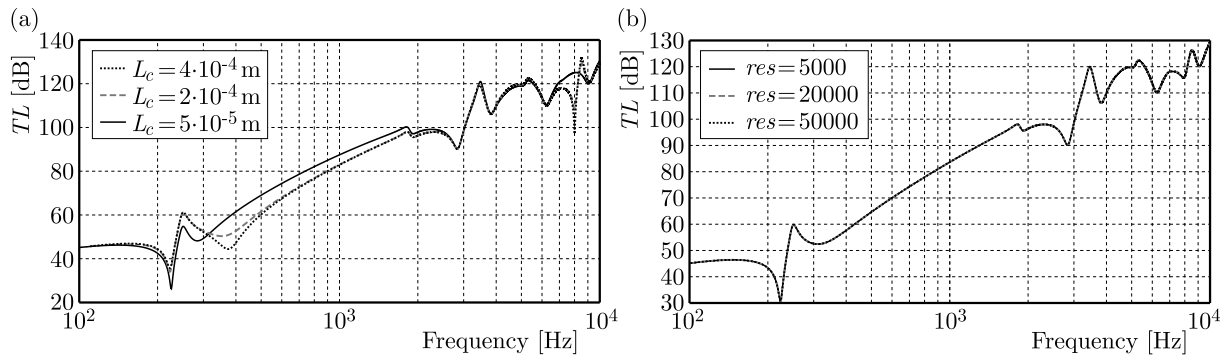

Fig. 11. Influence of (a) porous characteristic length and (b) flow resistivity on TL of the viscoelastic-porous-elastic configuration
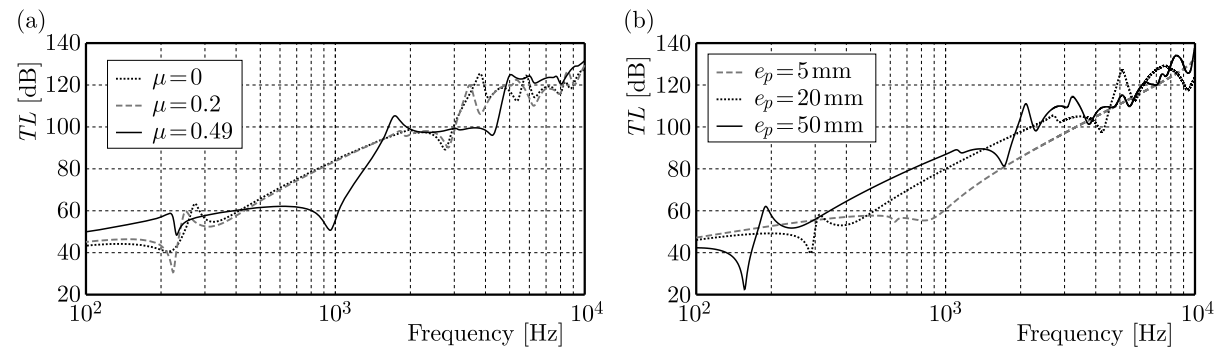

Fig. 12. Influence of (a) porous Poisson's ratio and (b) thickness of the porous material on TL of the viscoelastic-porous-elastic configuration

5. Conclusion

This article investigates the loss of sound transmission in multilayer configurations composed of porous, elastic and viscoelastic materials. A transfer matrix method has been developed to predict the acoustic behavior of a multilayer panel. The results were compared with experiments found in the literature. A comparison was made between all the configurations in order to find the best structure of the multilayer panel in terms of sound insulation. This comparison shows the effect of the damping of the viscoelastic layer which increases the loss of transmission (TL) as a function of the frequency.

Numerical simulations have been carried out to study the effects of porous parameters on the transmission loss for the best chosen configuration (viscoelastic-porous-elastic). This parametric study shows that porous material parameters like Young's modulus, Poisson's ratio and its thickness have a clear influence on the loss by transmission. The observed results are very useful for researchers and developers.

References

1. ABID M., ABBES J.D., CHAZOT L., HAMMAMI M.A., HAMDI, HADDAR M., 2012, Acoustic response of a multilayer panel with viscoelastic material, *International Journal of Acoustics and Vibration*, **17**, 2, 82-89

2. ALLARD J.F., ATALLA N., 2009, *Propagation of Sound in Porous Media. Modeling Sound Absorbing Materials*, Second Edition, John Wiley & Sons

3. ALLARD J.F, CHAMPOUX Y., DEPOLLIER C., 1987, Modelization of layered sound absorbing materials with transfer matrices, *Journal of the Acoustical Society of America*, **82**, 1792-1796

4. ALLARD J.F., DEPOLLIER C., REBILLARD P., LAURIKS W., COPS A., 1989, Inhomogeneous Biot waves in layered media, *Journal of Applied Physics*, **66**, 2278-2284

5. ATALLA N., PANNETON R., DEBERGUE P., 1998, A mixed displacement pressure formulation for poroelastic materials, *Journal of the Acoustical Society of America*, **104**, 1444-1452

6. BIOT M.A., 1956, The theory of propagation of elastic waves in a fluid satured porous solid, *Journal of the Acoustical Society of America*, **28**, 68-191

7. FOLDS D.L., LOGGINS D.C., 1977, Transmission and reflection of ultrasonic waves in layered media, *Journal of the Acoustical Society of America*, **62**, 1102-1109

8. GHINET S., ATALLA N., HAISAM O., 2005, The transmission loss of curved laminates and sandwich composite panels, *Journal of the Acoustical Society of America*, **118**, 774

9. LEE C.M, XU Y., 2009, A modified transfer matrix method for prediction of transmission loss of multilayer acoustic materials, *Journal of Sound and Vibration*, **326**, 290-301

10. LONDON A., 1950, Transmission of reverberant sound through double walls, *Journal of the Acoustical Society of America*, 220-270

11. MUNJAL M.L., 1993, Response of a multi-layered infinite plate to an oblique plane wave by means of transfer matrix, *Journal of Sound Vibration*, **162**, 2, 333-343

12. MUELLER P., TSCHUDL H., 1989, Modeling of flat multi-layer acoustic structures with transfer matrices, *SAE Technical Paper*, 111-115

13. SASTRY J.S., MUNJAL M.L., 1995, A transfer matrix approach for evaluation of the response of a multi-layer infinite plate to a two-dimensional pressure excitation, *Journal of Sound and Vibration*, **182**, 1, 109-128

14. SOULA M., CHEVALIER Y., 1998, The fractional derivative in rheology of polymers – application to the elastic and viscoelastic behavior of linear and nonlinear elastomers, *ESAIM Proceedings*, **5**, 87-98

15. Szabo T.L., 2000, A model for longitudinal and shear wave propagation in viscoelastic media, *Journal of the Acoustical Society of America*, **107**, 5, 2437-2446

16. Tanneau O., 2004, Modélisation de panneaux d'isolation aéronautiques – couplages poroélastique, élastodynamiques et acoustiques par méthodes analytiques, FEM et BEM: Phd Thesis, Université Pierre & Marie Curie, Paris VI

17. Tanneau O., Casimir J.B., Lamary P., 2006, Optimization of multilayered panels with poroelastic components for an acoustical transmission objective, *Journal of the Acoustical Society of America*, **120**, 3, 1227-1238

18. Thomson W.T., 1950, Transmission of elastic waves through a stratified solid medium, *Journal of Applied Physics*, **21**, 2, 89-93